Heterogeneous deformation and recrystallisation of iron base oxide dispersion strengthened PM2000 alloy

C. Capdevila, Y. L. Chen, N. C. K. Lassen, A. R. Jones, and H. K. D. H. Bhadeshia

The recrystallisation behaviour of PM2000 oxide dispersion strengthened ferritic alloy has been investigated for tube specimens which had been cold deformed after extrusion. The evolution of the recrystallisation temperature, defined as the minimum temperature at which the specimen begins to recrystallise, has been studied in detail as a function of the level of deformation. The microstructure was characterised using optical and transmission electron microscopy, together with microhardness measurements, and local texture measurements obtained using the electron backscattering pattern technique. The results can be interpreted if it is assumed that any procedure that produces a heterogeneous microstructure, stimulates recrystallisation. In this sense, larger strain gradients lead to more refined and more isotropic grain structures. The way in which these results can be exploited for commercial applications is discussed. **MST/4742**

Dr Capdevila and Professor Bhadeshia are in the Department of Materials Science and Metallurgy, University of Cambridge, Pembroke Street, Cambridge CB2 3QZ, UK (www.msm.cam.ac.uk/phase-trans). Dr Chen and Dr Jones are in Materials Science and Engineering, Faculty of Engineering, University of Liverpool, L69 3GH, UK (www.liv.ac.uk/mateng/home.html). Dr Lassen is in the Materials Research Department, Risø National Laboratory, DK–4000 Roskilde, Denmark (www.risoe.dk).
Manuscript received 19 June 2000; accepted 12 September 2000.

Introduction

There is a commitment in Europe to renewable energy; biomass is likely to make a significant contribution to this type of power generation.[1] This does not require radically new technologies when compared with alternative sources of renewable energy. However, the thermodynamic efficiency of the process is dependent on the maximum temperature which can be attained in the operating cycle. Technologies for developing biomass plant towards greater efficiencies are therefore vital. For example, it is planned to construct a heat exchanger capable of gas operating temperatures and pressures of around 1100°C and 15–30 bar. This in turn requires metal tubing which can withstand temperatures up to 1150°C.

Mechanical alloying is a process in which different powder mixtures are deformed to such an extent that a solid solution is formed.[2] Stable oxides can also be incorporated into the alloy during this process.[3,4] Alloys produced in this way are available on a commercial scale and have many applications.[5–7]

The oxidation resistance and good creep performance of mechanically alloyed iron base oxide dispersion strengthened (ODS) alloys, such as PM2000 and MA956, makes them prime candidates for the proposed heat exchangers.[8,9] As expected, the creep strength is influenced by grain size and shape.[10] Only coarse recrystallised grains have adequate high temperature creep strength. The microstructure following mechanical alloying and consolidation of the resulting powder (for example, by extrusion) consists of fine grains, much less than a micrometre in width, which are cold deformed during the consolidation process.[11–14] The material in this state is hard and contains very high levels of stored energy.[15,16] Therefore, it has to be recrystallised into a coarse grained microstructure before use. However, the recrystallisation behaviour of iron base ODS alloys is peculiar in that they recrystallise into a grain structure which resembles that obtained by directional solidification, with coarse, columnar grains having their longest axis along the extrusion direction. Furthermore, recrystallisation usually does not occur until temperatures close to melting are reached.[17–19]

Although the coarse and directional grain structure is ideal for minimising creep along the axis of the columnar grains, the properties in the transverse direction are less than desired. For this reason, there is considerable interest in controlling the development of microstructure. Many of the methods which seek to alter the microstructure rely on some type of deformation of the consolidated metal before the recrystallisation heat treatment. Regle and Alamo[20] studied the influence of cold deformation on the recrystallisation and obtained fascinating results in which the recrystallisation temperature and grain structure were radically altered by the degree of deformation.

The purpose of the work presented in this paper was to study the effect of a non-uniform deformation on the recrystallisation behaviour of PM2000 so as to propose a method of producing coarse grain structures. PM2000 tubing is normally processed by unidirectional extrusion followed by heat treatment which produces the axially aligned microstructures. As would be expected, these exhibit excellent axial creep properties. However, in pressurised tubes, the stress is larger along the hoop direction where the creep strength is poorer. Therefore, analysis was undertaken of the effect of deformation induced by an unusual torsional extrusion process, known as flow forming, on the recrystallisation behaviour of tube specimens intended for the heat exchanger application.

Experimental procedure

The nominal composition of the PM2000 alloy used is Fe–20Cr–0·5Ti–5·5Al–0·5Y_2O_3 (all wt-%). PM2000 is produced by mechanical alloying of the components in a high energy mill to produce a solid solution which contains a uniform dispersion of yttria, in the form of coarse powder. The powder is then consolidated using hot isostatic pressing and the resulting tube preforms are then extruded. The alloy

was supplied by Plansee GmbH. The essential feature of PM2000 is that it contains 5·5%Al and 0·5%Y_2O_3. The aluminium enhances corrosion and oxidation resistance and it is claimed that PM2000 is better than other ODS materials in gaseous environments containing N_2–0·24%SO_2–15%CO_2–4%O_2.[21,22] The creep performance has been found to be optimum with a Y_2O_3 content of 0·5%.

In an attempt to produce microstructures which optimise the creep strength along the hoop direction, a novel processing route of flow forming, developed at Metall-Spezialrohr GmbH (MSR), was used to produce experimental tubes. Flow forming is a process of chipless manufacture, in which the material of the tube is subjected to compressive stress between a mandrel (located inside the tube) and three work rollers located symmetrically around its circumference. Owing to the proprietary design of the rollers, the tube not only extends but also twists, the total deformation being a combination of torsion and extrusion.

It is well established[12,13] that the yttria particles in iron base mechanically alloyed materials are aligned along the extrusion direction, probably because the powder particles used in the feedstock do not always contain identical quantities of yttria. Thus, on extrusion, they tend to align along the elongation direction of the particles, which in this case is also the extrusion direction. The purpose of this torsional deformation is to cause these axially aligned particles to turn into helical arrangements in the hope that the material will then recrystallise into grains which twist along the extrusion axis and hence give better hoop strength. However, the twisted grain structure is not discussed in this paper, simply the effect of flow forming on the development of microstructure.

The extruded tubes from Plansee were flow formed by the process of torsional extrusion at room temperature, which led to reductions in wall thickness of from 4 to 1·4 mm, tube T1, and from 4 to 0·6 mm, tube T2. (Initial o.d. and i.d. were 53·5 and 49 mm respectively.) Throughout this work, the two tubes T1 and T2, which have different levels of reduction in area (RA), i.e. 72 and 90% respectively, were studied.

Samples for metallographic examination were cut from the transverse direction of the tube. Optical microscopy was used to observe the microstructures of both as flow formed and heat treated specimens. The etchant used was 2 g $CuCl_2$, 40 ml HCl, and 40–80 ml ethanol. Transmission electron microscopy was carried out using a JEOL 2000FX microscope operated at 200 kV to evaluate the deformed microstructure in flow formed tubes. To minimise any defects introduced by sample preparation, foils were extracted by spark erosion. Samples were ground and polished to about 30–50 μm thickness, then thinned to perforation by ion milling.

Vickers microhardness measurements were carried out in as flow formed samples by means of a Mitutoyo Mvk-H2 hardness tester machine with a load of 200 g.

The crystallographic textures of tubes T1 and T2 were investigated using the electron backscattering pattern (EBSP) technique. This technique allows rapid, automated measurements of crystal orientations with high precision ($<1^\circ$) and high spatial resolution (<100 nm) in the SEM. In this study, the technique was used for measuring local textures on the outer surface, in the middle, and on the inner surface of the tubes.

The sample preparation for local texture measurements using EBSP is described as follows. A slice of approximately 15 mm was cut from both tube T1 and tube T2. Each ring slice was then cut into 12 samples of size $\sim 15 \times 5$ mm (the third dimension being the thickness of the tube), as shown in Fig. 1. The 12 samples were taken from positions well spaced over the circumference of the ring, as illustrated in Fig. 1*b*. Samples of each tube were prepared for EBSP analysis using mechanical grinding and polishing followed by electropolishing (A2 electropol). For all the samples, the plane investigated by EBSP was that containing the tube axis (TD) and the radial direction (RD), as illustrated in Fig. 1*a*.

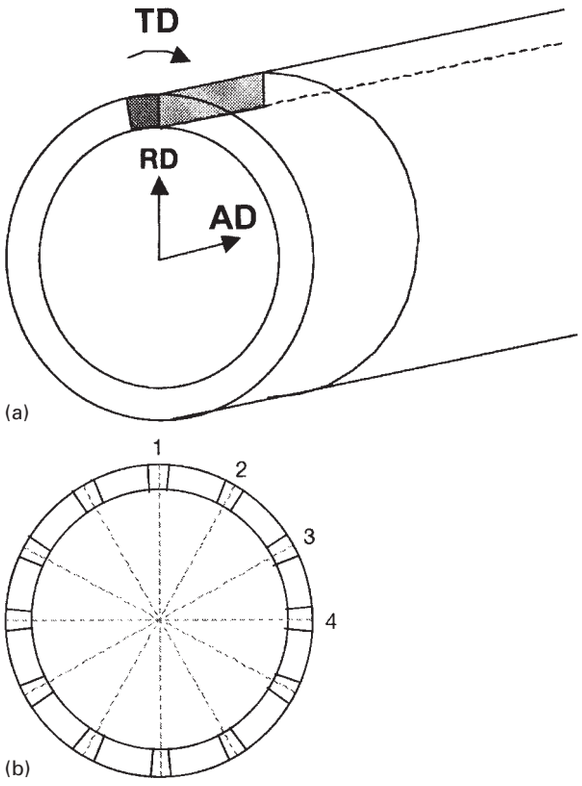

1 *a* schematic diagram of geometry of samples cut from tubes for EBSP measurements (plane investigated by EBSP contains TD and RD) and *b* location on ring slice of 12 samples cut for EBSP investigation

To obtain the EBSPs, two or three samples were mounted on a special holder and inserted into a JEOL JMS840 SEM equipped with a LaB6 filament. The accelerating voltage was either 15 or 20 kV and the beam current 1–2 nA. The EBSPs were recorded on a high quality detector from Nordif and analysed with specialised software developed at the Risø National Laboratory. Local textures were made by performing linescans in the tube direction (TD) across the entire sample. The total distance covered by each linescan was about 15 mm and the distance between sampled points chosen varied from 35 to 150 μm. Typically, 100–400 orientations where measured on each linescan. Linescans made near the outer surface and near the inner surface of the tubes were made at a distance of approximately 100 μm from the edges.

The crystal orientation (texture) data were represented as (100) pole figures which show the stereographic projection of {100} planes in the crystals onto the TD–RD plane.

Recrystallisation temperature T_R

The temperature T_R is defined as the minimum temperature at which optical microscopy indicates some signs of recrystallisation following 1 h of heat treatment. Measured values of T_R for the inner and outer surfaces of the tubes are respectively 1190 and 835°C for T1 (72% RA) and 1200 and 1175°C for T2 (90% RA). Tube T2 shows uniform behaviour, whereas the T_R of the outer surface of T1 is much less than that of the inner surface. Furthermore, the recrystallisation behaviours of T1 and T2 are found to be quite different. In tube T1, recrystallisation begins close to

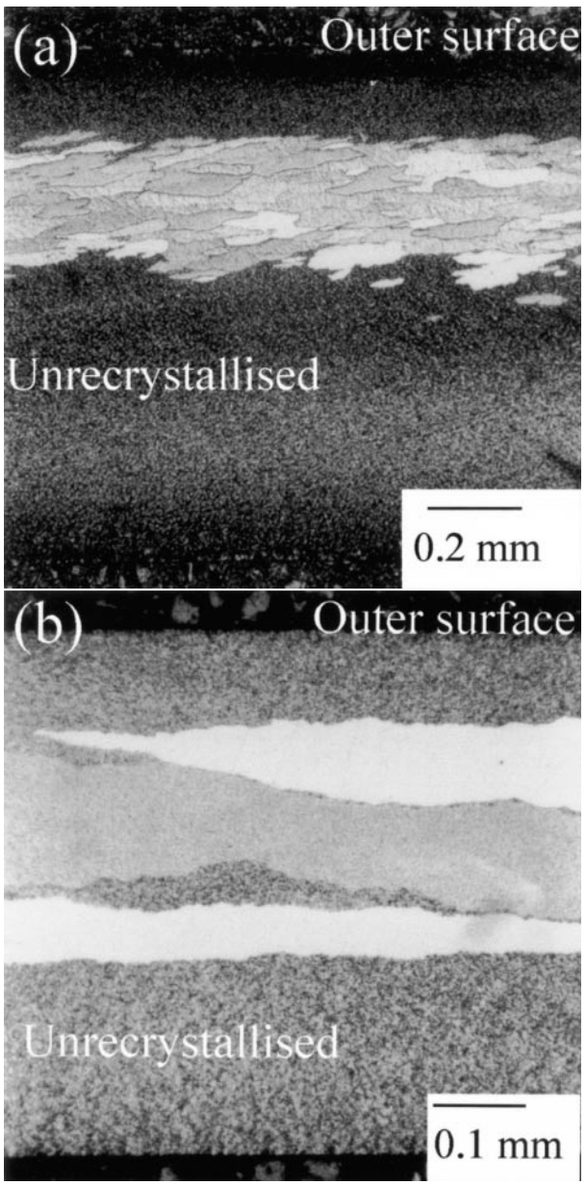

2 Transverse sections of *a* tube T1 recrystallised at 870°C for 30 min and *b* tube T2 recrystallised at 1180°C for 1 h

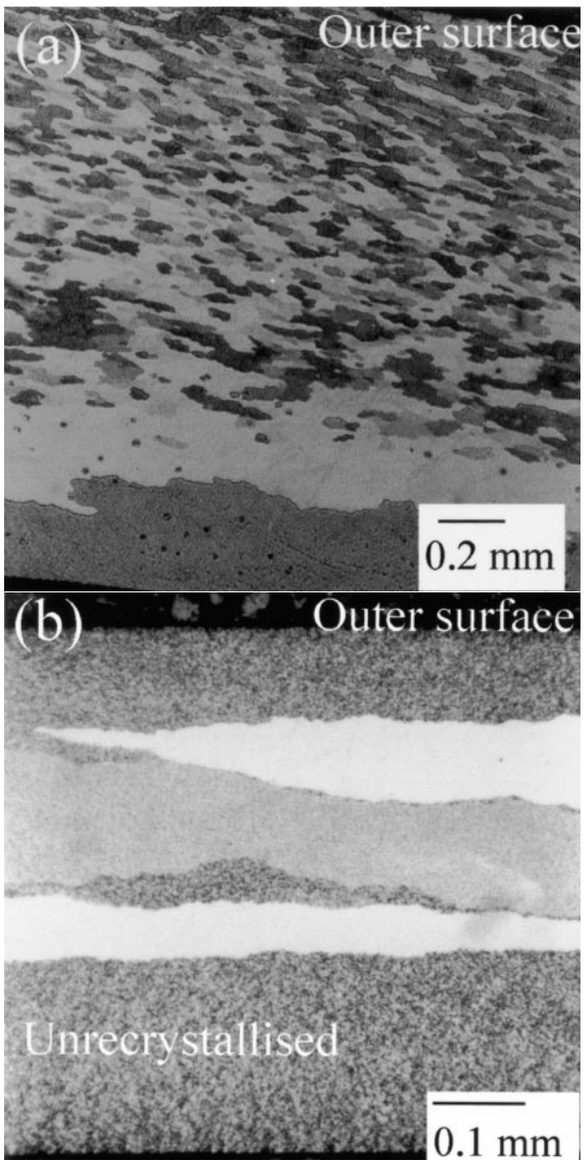

3 Transverse sections of *a* tube T1 and *b* tube T2 both recrystallised at 1380°C for 1 h

the outer surface (Fig. 2*a*), whereas it initiates in the centre of the T2 (Fig. 2*b*). Moreover, the shapes of the recrystallised grains are very different in the two tube materials. More refined and equiaxed grains are obtained after recrystallisation in T1 when compared with T2, as is shown in Fig. 3.

Surface per unit volume S_V

Given the columnar grain structure, the surface per unit volume of recrystallised grain boundary was measured according to Bhadeshia *et al.*[23] Thus, the columnar grains were approximated as space filling hexagonal prisms of cross-sectional side length a and height c, where $c \gg a$. Since the recrystallised microstructure in PM2000 is anisotropic because the grain growth velocity is much higher along the extrusion direction, the final recrystallised grains can be also approximated as space filling hexagonal prisms. The mean linear intercept as measured on random sections is then given by

$$\bar{L} = \sqrt{12}\,\frac{ac}{2c+\sqrt{3}a} \quad \ldots\ldots\ldots\ldots\ldots\ldots \quad (1)$$

For $c \gg a$, this becomes

$$\bar{L} = a\sqrt{3} \quad \ldots\ldots\ldots\ldots\ldots\ldots \quad (2)$$

The three different sections examined in the present work are shown in Fig. 4. Linear intercept measurements were carried out from montages of micrographs taken at magnifications ranging from $\times 50$ to $\times 100$. The low magnification is necessary in order to ensure sufficient numbers of complete sections of recrystallised grains in the area examined. For directional microstructures, the linear intercept is a function of scan orientation relative to the microstructure, whereas equations (1) and (2) require that the test lines be randomly orientated with respect to the microstructure. Hence, each field was studied at 15 orientations of the scan direction.

Mean lineal intercept measurements from the two longitudinal sections L_{L1} and L_{L2} and the transverse

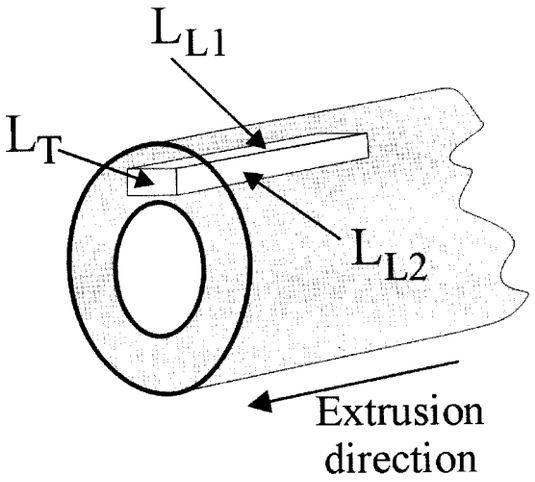

4 Schematic diagram of sections on which stereological measurements were carried out

section L_T are given in Table 1. The errors in the measurements are due to the finite number N of tests and to the variability in the size of features, as expressed by the standard deviation σ. Both of these effects can be taken into account by calculating the standard error (SE) of the mean, given by[24]

$$\mathrm{SE} = \frac{\sigma}{\sqrt{N}} \quad \ldots \quad (3)$$

Figure 5 shows the evolution of the surface per unit volume ($S_V = 2/\bar{L}$) for the recrystallised grains as a function of deformation. With increasing deformation, the grain shape tends to become more elongated and the grains also increase in length, leading to the smaller intercepts for T2.

Grain aspect ratio

The good high temperature properties of ODS materials correlate directly with their coarse elongated grain structures. The grain aspect ratio (GAR) of a material can be expressed as follows

$$\mathrm{GAR} = \frac{(L_{L1}L_{L2})^{1/2}}{L_T} \quad \ldots \quad (4)$$

The grain structure developed in PM2000 can vary from

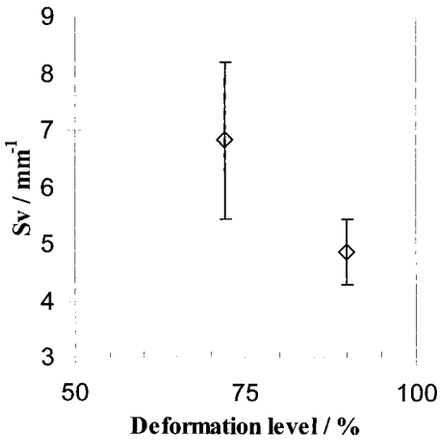

5 Evolution of recrystallised grain surface per unit volume S_V as function of degree of deformation for PM2000

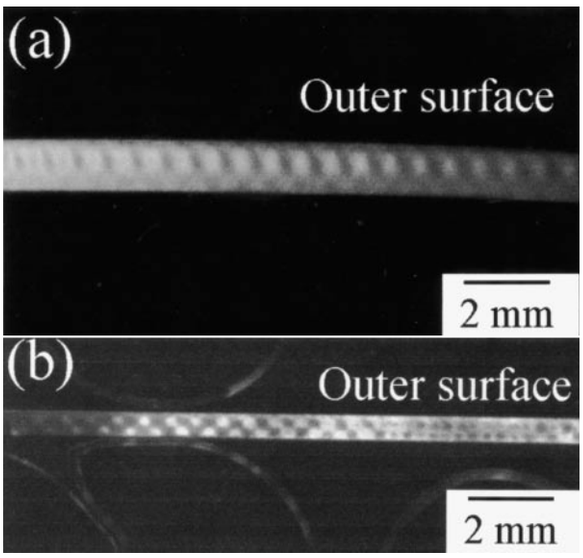

6 Transverse sections of *a* tube T1 and *b* tube T2 showing pattern of flow forming deformation

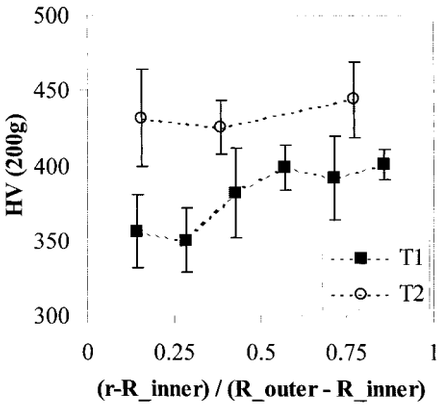

7 Comparison of strain gradient across wall thickness of tube T1 and tube T2: *R*_outer is initial outer radius of tubes, *R*_inner is inner radius which remains constant, *r* is radial coordinate

micrometre sized grains to structures with high grain aspect ratios. The measured grain aspect ratios for recrystallised grains as a function of degree of deformation are: 6 ± 2 and 12 ± 3 for T1 (72% RA) and T2 (90% RA) respectively.

Through thickness strain distribution

During flow forming, the surface of the tube is in contact with the rollers whereas the interior is in contact with a stationary mandrel. The torsional influence of the rollers

Table 1 Mean linear intercept measurements $\bar{L} = (L_T + L_{L1} + L_{L2})/3$ for recrystallised grain structures: standard error (SE) values for $\bar{L}$ are calculated from means of SE values for three different sections studied

Tube	$\bar{L}_T$, mm	$\bar{L}_{L1}$, mm	$\bar{L}_{L2}$, mm	$\bar{L}$, mm	σ	SE
T1	0·067	0·381	0·431	0·293	0·059	0·024
T2	0·048	0·589	0·595	0·411	0·048	0·019

σ is standard deviation.

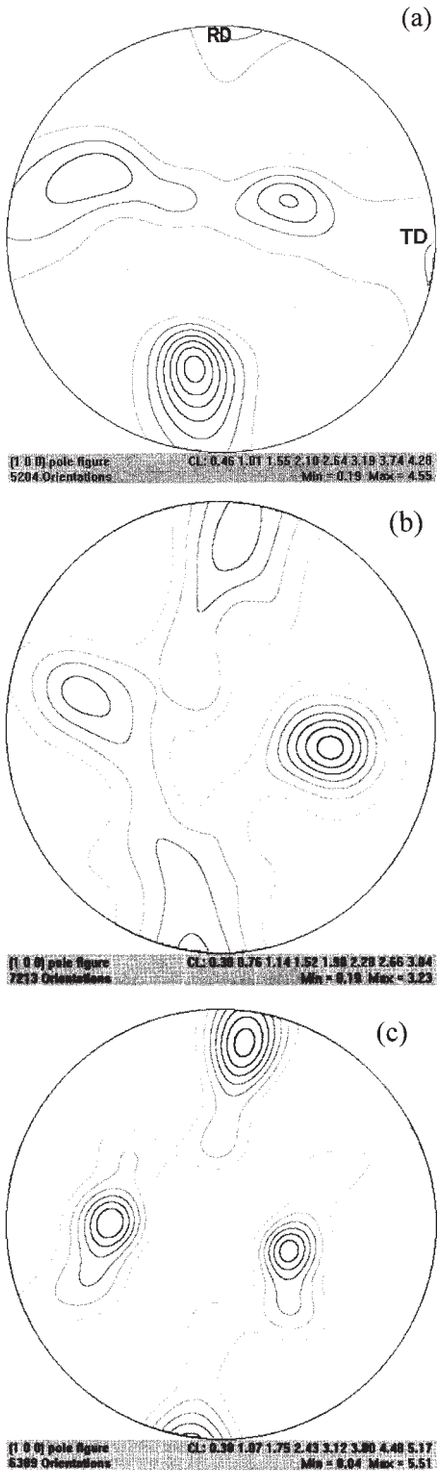

a outer surface: fibre texture (RD=[100]); *b* centre: random; *c* inner surface: rotated cube (TD=[110]; RD=[001])

8 Texture of tube T1 before heat treatment

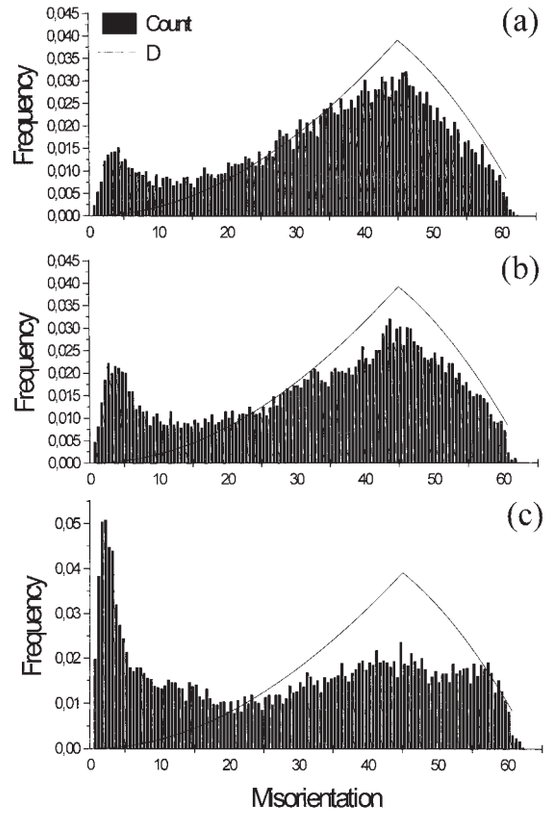

a outer surface; *b* centre; *c* inner surface

9 Misorientation distribution of tube T1 before heat treatment

does not therefore penetrate effectively through the thickness of the tube when the reduction in wall thickness is small. Figure 6 illustrates this phenomenon: the cross-sectional unetched image of tube T1 reveals a periodicity in the image of the upper half of the wall thickness, corresponding to the effect of the rollers. By contrast, the lower half of the wall thickness has a uniform appearance due to its contact with the mandrel. Tube T2, on the other hand, with its larger reduction in thickness, shows the effect of the rollers through the entire section. Note that the periodic contrast is on unetched, polished samples and reflects the state of residual stress in the material. It is the relaxation of the stress at the surface which gives rise to the contrast in an optical microscope. To summarise, the deformation is more uniform through the thickness of the tube for the larger reduction in wall thickness.

That the overall deformation is less homogeneous in tube T1 than in tube T2 is confirmed by the data presented in Fig. 7, which shows the evolution of the hardness across the wall thickness of the two tubes. The hardness distribution for T2 is clearly more homogeneous than for T1.

The crystallographic texture has also been measured as a function of depth in the deformed tube (Fig. 8). The outer surface of tube T1 has a fairly strong fibre texture with axis RD=[100]. By contrast, the centre of the tube has a weak almost random texture. The inner surface shows a strong texture dominated by a rotated cube component (TD=[110]; RD=[001]). The misorientation distributions are illustrated in Fig. 9. The orientations have been measured on a rectangular grid with a sampling distance of 1 μm between grid points by means of electron backscatter diffraction. The y axis shows the normalised counts of misorientations (a rotation angle between 0 and 62·8° for cubic crystals) between neighbouring grains which fall within the selected intervals of 0·5°. The solid line on the histograms shows the distribution for randomly oriented crystals (Mackenzie distribution). From this figure, it can be concluded that there is an increase in the fraction of low angle boundaries towards the inside of the tube (Fig. 9).

The texture results of tube T2 are shown in Fig. 10. The three textures from the outer surface, centre, and inner surface all show a maximum where RD=[100]. Three ideal orientations dominate the texture: rotated cube (101)[110], and $(1\bar{1}1)[1\bar{1}0]$ and $(111)[1\bar{1}0]$. The textures become stronger

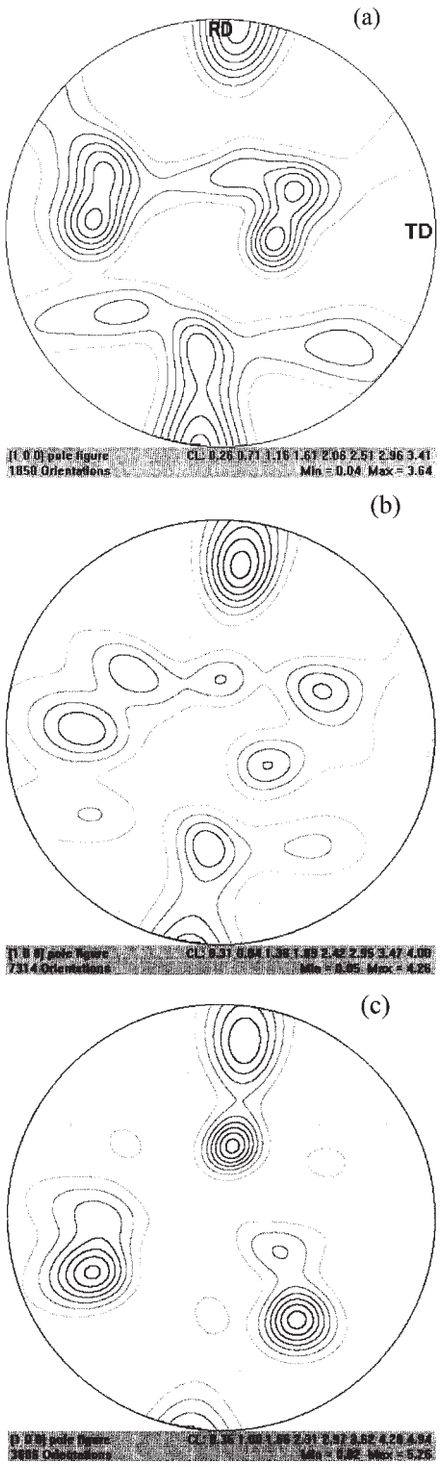

a outer surface: weak peaks between rotated cube (101)[110] and $(1\bar{1}1)[1\bar{1}0]$; *b* centre: peaks around rotated cube (101)[110] and (111)[$\bar{1}$10] and $(\bar{1}11)[1\bar{1}0]$; *c* inner surface: strong peaks at rotated cube (101)[110] and $(111)[1\bar{1}0]$

10 Texture of tube T2 before heat treatment

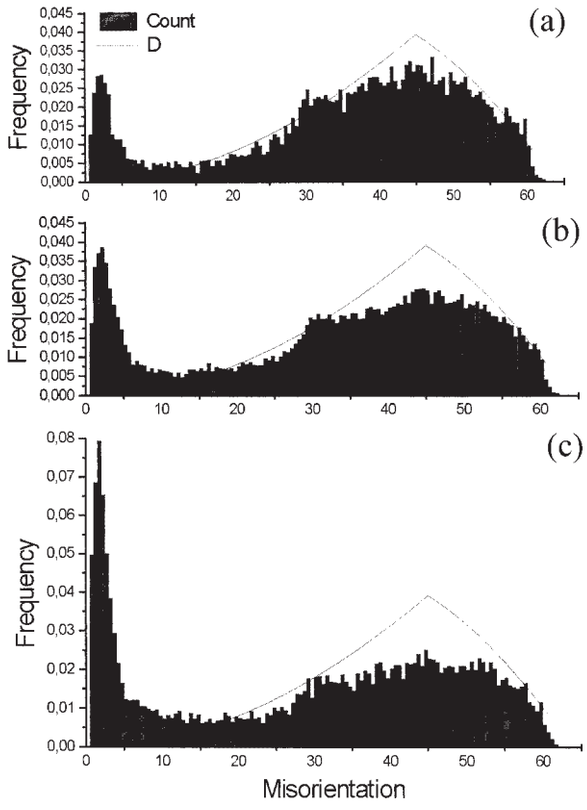

a outer surface; *b* centre; *c* inner surface

11 Misorientation distribution of tube T2 before heat treatment

when moving from the outer surface towards the inner surface. Near the outer surface, the texture is fibre-like (fibre axis RD = [100]). The fibre tendency decreases towards the inside.

There are similarities in the texture results of tubes T1 and T2: rotated cube component, fibre-like on the outer surface, strong texture on the inner surface. There are also differences: the $(1\bar{1}1)[1\bar{1}0]$ and $(111)[1\bar{1}0]$ components are not clearly observed in T1. Similarly, T2 shows a steady increase in texture strength from outside to inside, whereas T1 has a fairly weak texture in the centre. In general, it can be concluded that the texture is more homogeneous over the tube thickness for T2. This, of course, is expected given the more homogeneous distribution of strain in T2.

Histograms of the misorientation distribution across the wall thickness of tube T2 (Fig. 11) show an increase in the number of low misorientation boundaries on moving from the outer towards the inner surface. The change from the outer surface to the centre is only minimal, but the change from centre to inner surface is quite significant. Comparing the data with that from tube T1 reveals several differences. For all layers, the shape of the histogram is quite different. In particular, the distribution of the low misorientation boundaries ($<15°$) is more concentrated at the very low misorientations ($<3°$) for T2 than for T1 which has a more evenly spread distribution. For all layers, the fraction of boundaries with less than 3° misorientation is significantly larger for T2 than for T1. This concentration around very low angle boundaries seems to be the most pronounced difference found between T1 and T2 from the misorientation distributions.

Recrystallisation 'nucleates' by the bowing of grain boundaries. With the submicrometre grain size of mechanically alloyed metals, the grain junctions themselves act as severe pinning lines for grain boundary bowing.[25] The activation energy for the nucleation of recrystallisation is therefore very large, requiring exceptionally high recrystallisation temperatures. However, recrystallisation becomes much easier, and can occur at much lower temperatures, if a few grains happen to be slightly larger, i.e. if the grains are not uniform in size, or if there are local strain heterogeneities which assist nucleation.

Non-uniform strain must therefore enhance nucleation leading to a finer recrystallised grain size and a reduction in T_R, as is observed for tube T1. The same reasoning explains why T_R is high for T2, and why its grain structure is coarse in spite of the higher degree of deformation during flow forming.

The crystallographic texture results are also consistent with this interpretation. Li[26] reported that the diffusion of atoms between grains is more difficult when the grains are related by a low misorientation. A preponderance of low misorientation boundaries would therefore inhibit recrystallisation kinetics, including the motion of the grain boundary during the bowing stage of nucleation. The inner surface of the flow formed tube T1 has a high frequency of low misorientation boundaries; therefore, coarse grains are obtained on the inner surface of the tube when compared with the outer surface. Similarly, there must be an inhibition of nucleation in T2 due to high fraction of low misorientation boundaries which explains the coarse grained structure.

Conclusions

The influence of deformation on the recrystallisation of mechanically alloyed PM2000 has been studied. Tubes with two different levels of deformation due to flow forming have been studied. As the reduction in area increases, a more homogeneous submicrometre microstructure and strain gradient across the wall thickness of the tube is observed. Similarly, the differences between the minimum temperature at which recrystallisation in the outer and inner surface of the tube takes place is reduced as deformation increases.

The results from hardness testing and microstructural and crystallographic texture investigations are all consistent with the broad concept that any procedure which introduces heterogeneity into the microstructure, stimulates the nucleation of recrystallisation, giving a fine grained microstructure.

Acknowledgements

Two of the authors (CC and HKDHB) are grateful to Professor A. H. Windle for the provision of laboratory facilities at the University of Cambridge and the European Commission for funding the work via a Brite/Euram III project. It is a pleasure to acknowledge our project partners: Plansee GmbH, Metall-Spezialrohr GmbH (MSR), Sydkraft, and Mitsui Babcock Technology Centre.

References

1. D. J. GOOCH: Proc. 5th International Charles Parsons Turbine Conference, 1073–1093; 2000, London, IoM Communications.
2. J. S. BENJAMIN: *Metall. Trans.*, 1970, **1**, 2943–2951.
3. J. S. BENJAMIN and T. E. VOLIN: *Metall. Trans.*, 1974, **5**, 1929–1934.
4. P. S. GILMAN and J. S. BENJAMIN: *Ann. Rev. Mater. Sci.*, 1983, **13**, 279–300.
5. M. J. FLEETWOOD: *Mater. Sci. Technol.*, 1986, **2**, 1176–1182.
6. R. SUNDARESAN and F. H. FROES: *J. Met.*, 1987, **39**, 22–27.
7. V. C. NARDONE, D. E. MATEJCZYK, and J. K. TIEN: *Metall. Trans.*, 1981, **3A**, 141–145.
8. D. SPORER and K. LEMPENAUER: Proc. 13th International Plansee Seminar, 'Structural stability of ODS superalloys', (ed. H. Bildstein and R. Eck), 796–810; 1993, Reutte, Plansee.
9. F. STARR, A. R. WHITE, and B. KAZIMIERZA: Proc. Conf. 'Materials for advanced power engineering', (ed. D. Coutsouradis *et al.*), 1393–1411; 1994, Dordrecht, Kluwer.
10. F. G. WILSON, B. R. KNOTT, and C. D. DESFORGES: *Metall. Trans.*, 1978, **9A**, 275–287.
11. M. M. BALOCH: 'Directional recrystallisation in dispersion strengthened alloys', PhD thesis, University of Cambridge, 1989.
12. D. M. JAEGER and A. R. JONES: Proc. Conf. 'Materials for advanced power engineering', (ed. D. Coutsouradis *et al.*), 1507; 1994, Dordrecht, Kluwer.
13. D. M. JAEGER and A. R. JONES: Proc. Conf. 'Materials for advanced power engineering', (ed. D. Coutsouradis *et al.*), 1515; 1994, Dordrecht, Kluwer.
14. T. S. CHOU, H. K. D. H. BHADESHIA, G. MCCOLVIN, and I. C. ELLIOTT: Proc. 2nd Int. Conf. on 'Structural applications of mechanical alloying', 77–82; 1993, Materials Park, OH, ASM International.
15. T. S. CHOU and H. K. D. H. BHADESHIA: *Metall. Trans.*, 1993, **24A**, 773–779.
16. T. S. CHOU and H. K. D. H. BHADESHIA: *Mater. Sci. Technol.*, 1993, **9**, 890–897.
17. J. S. BENJAMIN and P. S. GILMAN: 'Metals handbook', 9th edn., Vol. 7, 722; 1983, Materials Park, OH, ASM International.
18. G. H. GESSINGER: 'Powder metallurgy of superalloys'; 1984, London, Butterworth.
19. G. A. J. HACK: *Powder Metall.*, 1984, **27**, 73–79.
20. H. REGLE and A. ALAMO: *J. Phys. (France) IV*, 1993, **C7–111**, 727–730.
21. H. D. HEDRICH: Proc. Conf. 'New materials by mechanical alloying techniques', (ed. E. D. Artz and L. Schultz), 217–230; 1986, Germany.
22. G. P. DEGAUDENZI, F. UBERTI, F. BREGANI, and G. P. TOLEDO: Proc. Conf. 'Materials for advanced power engineering', part 2, (ed. D. Coutsouradis *et al.*), 1563–1572; 1994, Dordrecht, Kluwer.
23. H. K. D. H. BHADESHIA, L.-E. SVENSSON, and B. GRETOFT: *J. Mater. Sci.*, 1989, **21**, 3947–3951.
24. E. E. UNDERWOOD: 'Quantitative stereology', 92; 1970, Reading, MA, Addison-Wesley.
25. H. K. D. H. BHADESHIA: *Mater. Sci. Eng.*, 1997, **A223**, 64–77.
26. J. C. M. LI: in 'Recovery and recrystallisation of metals', 160; 1960, London, Himmel.